Modeling of Coupled Physio-Chemical Processes of a Liquid Droplet between Two Contacting Porous or Non-Porous Materials

H. K. Navaz[1], A. L. Dang[2], A. R. Zand[3]

Abstract: A Computational model to solve the coupled transport equations with chemical reaction and phase change for a liquid droplet between two approaching porous or non-porous surfaces, is developed. The model is general therefore it can be applied to toxic chemicals (contact hazard), drug delivery through porous organs and membranes, combustion processes within porous material, and liquid movements in the ground. The equation of motion and the spread of the incompressible liquid available on the primary surface for transfer into the contacting surface while reacting with other chemicals (or water) and/or the solid substrate are solved in a finite difference domain with adaptive meshing. The comparison with experimental data demonstrated the model is robust and accurate. The impact of the initial velocity on the spread topology and mass transfer into the pores is also addressed.

Index Terms - Porous media, multi-component systems, CFD modeling of porous media, Chemistry in porous media

I. INTRODUCTION

The spread of a sessile liquid droplet between two porous or non-porous (substrates) surfaces in the presence of evaporation and chemical reaction with the substrate or other pre-existing liquids in the substrate is of great importance. A better understanding of all these coupled processes will help us to assess not only the environmental impact of disseminated chemicals in forms of industrial toxic waste, pesticides, or harmful agents, but also evaluate the threat by direct contact of such chemicals with other objects or skin. Generally, chemicals with higher vapor pressure pose a respiratory threat and those with lower vapor pressure will stay in substrates for a longer time and can be transferred to human skin or other objects by direct contact. However, some of these chemicals can enter a chemical reaction with some substrates, other pre-existing chemicals within a substrate, or moisture to become less and sometimes more toxic therefore altering their threatening characteristics. Our previous studies [1-13] have extensively focused on determining the capillary pressure function for a sessile droplet, the spread, and evaporation rate of a sessile droplet inside a porous substrate. A comprehensive literature search can be found in these references and will not be repeated here for brevity.

[1] Professor of Mechanical Engineering, Kettering University, 1700 University Blvd., Flint, Michigan 48504, email: hnavaz@kettering.edu
[2] Principal Scientist, Software and Engineering Associates (SEA), Inc., 1175 Fairview Drive, Suite I, Carson City, Nevada 89701
email: Anthony@seainc.com
[3] Professor of Chemsitry, Kettering University, 1700 University Blvd., Flint, Michigan 48504, email: azand@kettering.edu

In this manuscript, the focus will be on the chemical reaction, contact dynamics, and the amount of mass transfer from one substrate to the other for the duration of contact. The computer code developed during this research can be used to simulate many different scenarios involving capillary spread with chemical reaction.

II. MODEL

The contact of two approaching surfaces can be divided into three steps, schematically shown in Figure 1. The first step is the pre-contact phase where a sessile droplet is residing on a non-porous or porous surface referred to as the primary surface (PS). We refer to this liquid as the free volume liquid ($\forall_{free}$). The volume of liquid that is transported into the PS through the surface is ($\forall_{PS}$). The capillary transport of the liquid droplet into the PS will take place until the time of contact with the free volume liquid that may be present on the PS. The availability of this liquid depends on the transport properties of the PS and the time interval for the contact. If $\forall_{free} > 0$, the liquid droplet will be sandwiched between the two surfaces creating a liquid bridge. However, if there is no free liquid left on the surface at the time of contact, the transfer from the PS to the contacting surface (CS) will take place when the two surfaces touch. Upon a perfect contact, the value of saturation and its normal gradient in both media (zones) are assumed to be equal. This is usually referred to as "perfect contact" boundary condition. Similar boundary conditions can also be imposed on the contacting surfaces to obtain a numerical solution. When $\forall_{free} > 0$, the liquid bridge has the shape a hyperboloid with a decreasing height. The contact angle of this hyperboloid and the surfaces can be found through experiments. The remaining volume of the liquid bridge is calculated each time step after its capillary transport into the porous media. The separating distance is also calculated for each time step. By knowing the mass of the liquid bridge and its height, the contacting surface area (assumed to be circular) is updated in each time step. The rate of the radius increase will determine the spread rate.

The continuum formulation for the transport of a liquid sessile droplet into a porous medium is given by [2, 14, 15]. The equation of motion is added to the set and the coupled equations are given as:

ISBN: 978-988-19253-4-3
ISSN: 2078-0958 (Print); ISSN: 2078-0966 (Online)

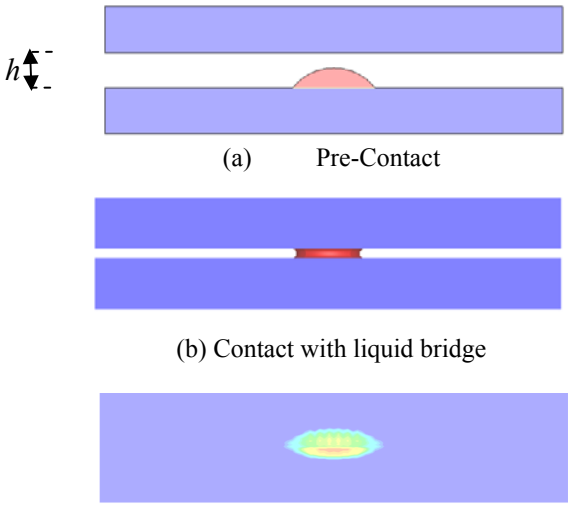

Figure 1: Schematics of pre-contact, contact, and post-contact phases.

Mass Conservation for Multiple Liquid System (Liquid "i")

$$\frac{\partial(\phi\rho_{\ell i}s_{\ell i})}{\partial t}+\nabla\bullet\left(\phi\rho_{\ell i}s_{\ell i}\vec{V}_{\ell i}\right)=-\dot{\rho}_{\ell i}^{\textbf{Secondary Evaporation}}-\dot{\rho}_{\ell i}^{\textbf{Surface Evaporation}}-\dot{\omega}_{\ell i}^{\text{Reaction}}-\dot{\omega}_{\ell i}^{\textbf{Adsorption}}$$

$$\rho_{\ell-\textbf{mixture}}=\sum_{i=1}^{N(\textbf{Liquids})}\rho_{\ell i}C_{\ell i}\qquad C_{\ell i}=\textbf{Mass Fraction}$$

Mass Conservation for Multiple Gaseous System (Gas "j")

$$\frac{\partial(\phi\rho_{gj}s_g)}{\partial t}+\nabla\bullet\left(\phi\rho_{gj}s_g\vec{V}_{gj}\right)=\nabla\bullet\left(\rho_g D_{j-mix}\nabla C_j\right)+\dot{\rho}_{\rho_{ii}}^{\textbf{Secondary Evaporation}}-\dot{\omega}_{gj}^{\text{Reaction}}-\dot{\omega}_{gj}^{\textbf{Adsorption}}$$

where: $s_g=1-\sum_{i}^{N(\textbf{Liquids})}s_{\ell i}$ and $\rho_g=\sum_{j=1}^{M(\textbf{Gases})}\rho_{gj}$

D_{j-mix} = ***Effective Diffusion Coefficient of gas species "j" into the mixture***

C_j = ***Mass Fraction*** $=\dfrac{\rho_{gj}}{\rho_g}$

Mass Conservation for Multiple Solid System (Substrate - Solid"k")

$$\frac{\partial\rho_{sk}\phi_s}{\partial t}=-\dot{\omega}_{sk}^{\text{Reaction}}-\dot{\omega}_{sk}^{\textbf{Adsorption}}$$

$$\phi_s=1-\phi$$

Momentum Equations:

$$\vec{V}_{\ell i}=-\frac{Kk_{\ell i}}{\mu_\ell}\left(\nabla P_{\ell i}-\rho_{\ell i}gs_{\ell i}\right)$$

$$\vec{V}_{gj}=-\frac{Kk_{gj}}{\mu_j}\left(\nabla P-\rho_{gj}gs_{gj}\right)-D_{j-Mix}\nabla C_j$$

ρ and μ are the density and viscosity of the gas mixture, respectively

$P_{\ell i}=P-P_{ci}$ (Capillary) $+\rho_{\ell i}gh^*$,

h^* = Local height of the droplet as a function of time (hydrostatic pressure)

$\dot{\omega}$ = ***Inter – Phase Chemical Species production or destruction***

K = ***Saturation permeability***

$k_\ell=k(s_\ell)$ Relative permeability is a function of the local saturation $=s_\ell^2$

$\phi=\phi(\rho_{sk},x,y,z)$ Local porosity is a function of ***local density*** of the solid phase

C = Mass Fraction

$k_{gj}=1+s_\ell^2(2s_\ell-3)$

(1)

In these equations "s" is the saturation, ϕ is the local porosity, ρ is the density, P is the pressure (the subscripts "ℓ" and "g" refer to liquid and gaseous phases, respectively), $\vec{V}_{\ell i}$ represents the velocity of "ith" liquid constituent and $\vec{V}_{jg}$ is the velocity of gaseous species "j".
The values without the subscript i and j represent the mass averaged mixture velocity for each phase. Capillary pressure is $P_c=P-P_\ell$, and effective diffusion coefficient $D_{j\text{-}Mix}$ is given in [2, 3] as:

$$D_{j-mix}=\{-0.5855(1-s_{\ell i})^3+0.4591(1-s_{\ell i})^2+0.1264(1-s_{\ell i})\}\phi(x,y,z,t)D_M$$

(2)

D_M represents the molecular diffusivity as a function of $T^{1.5}$ according to Trayball [16]. The liquid evaporation rate is $\dot{\rho}_\ell$ that is a sink term in the liquid phase equation and a source term in the vapor phase equation. $\dot{\omega}$ is the species production/destruction term.

The capillary pressure is given in [13] as:

$$f_i(*)\frac{\sigma_i\cos\theta_{mi}}{\sqrt{K_i/\phi}(x,y,z,t)}1.417(1-s_{\ell i})-2.120(1-s_{\ell i})^2+1.263(1-s_{\ell i})^3$$

(3)

Where σ_i is the surface tension for liquid species "i" and θ_{mi} is the contact angle inside the pores for liquid species "i" (usually taken to be zero). $f_i(*)$ will be determined experimentally according to the method outlined in [13]. The nominal value is usually about 0.1.

ISBN: 978-988-19253-4-3
ISSN: 2078-0958 (Print); ISSN: 2078-0966 (Online)

$$\text{Equation of Motion: } y = \frac{F}{2m}t^2 + V_O t + y_O$$

y = Coordinate system (Vertical),

V_O = Initial Velocity

y_O = Initial space between the two surfaces

F = Force exerted on the upper surface

m = mass of the upper surface

(4)

For this work we have not included the energy equation for brevity and will focus on isothermal processes. Equations (1) were transformed into the computational domain [$\xi=\xi(x,y,z)$, $\eta=\eta(x,y,z)$, $\zeta=\zeta(x,y,z)$] and marched in time to obtain the saturation function. The explicit fourth-order Runge-Kutta scheme was used to solve for the saturation.

The continuity and momentum equations are numerically integrated in time to find the distribution of liquid droplet inside the pores. At the boundary between the droplet and the porous substrate the saturation is unity ($s_\ell = 1$) and the capillary pressure is enhanced by the local hydrostatic pressure (based on local height, h^* in Fig. 1a) as: $P_\ell = P - P_{ci} + \rho_\ell g h^*$. Mass is being transported into porous medium according to $\frac{\rho_\ell \tilde{\upsilon}\phi}{J}$ where J is the Jacobian for the transformation and $\tilde{\upsilon}$ is the contra-variant vertical velocity given by: $\tilde{\upsilon} = \eta_x u + \eta_y \upsilon + \eta_z w$ with u, υ, w being the three components of the velocity and η_x, η_y, η_z being the metrics for the transformation. The mass transfer is calculated in each time step and the instantaneous remaining mass yields the liquid bridge volume. The volume of the hyperboloid was derived by deducting the volume of a "partial" torus from a cylinder with the base radius of r (liquid footprint) and height h using the Pappus second Theorem. The equation correlating instantaneous $r(t)$ and $h(t)$ with the liquid volume $\forall_{Liquid\ \ Bridge}(t)$ can be obtained as:

$$r^2(t) - \frac{h(t)G(\beta)}{4\cos^2\beta}r(t) - \frac{h^2(t)G(\beta)\tan\beta}{8\cos^2\beta} + \frac{h^2(t)}{6} - \frac{\forall_{Liquid\ \ Bridge}}{\pi h(t)} = 0$$

$$G(\beta) = \pi - 2\beta - \sin(\pi - 2\beta)$$

(5)

β is the contact angle between the surface and the liquid bridge. The droplet base radius (footprint), $r(t)$ is calculated from the above equation. As the gap between the two surfaces is closing the height will reduce. At the same time, the liquid is absorbed into the porous media. Therefore, $h(t)$ and $\forall_{Liquid\ \ Bridge}(t)$ are updated in each time step and the spread rate $\frac{dr(t)}{dt}$ can be obtained. Note that the $h(t)$ is determined by the equation of motion during this phase. Furthermore, when the height of the liquid bridge becomes less than a threshold, the spread is stopped. This threshold is a function of surface roughness and viscosity of the fluid, and can also be determined experimentally. At this point the radius of the footprint remains constant and the absorption is driven solely by capillary pressure causing a reduction in $h(t)$. This value of $h(t)$ can be calculated by solving the above equation again with the "final" liquid footprint radius. This equation is given as:

$$\left(\frac{\pi}{6} - \frac{\pi G(\beta)\tan\beta}{8\cos^2\beta}\right)h^3(t) - \frac{\pi r(t)G(\beta)}{4\cos^2\beta}h^2(t) + \pi r^2(t)h(t) - \forall_{Liquid\ \ Bridge} = 0$$

(6)

This will be a cubic equation in $h(t)$. As the absorption into the porous media occurs, the volume of the droplet is updated and the new $h(t)$ is calculated.

It should be noted that the time required for the topology of a sessile droplet (Figure 1a) to change to a liquid bridge (Figure 1b) is estimated to have a magnitude of $O(r_o^2\mu/\sigma z_o)$ where r_o and z_o are characteristic lengths in vertical (direction of motion) and radial (direction of spread) directions, respectively. μ is the viscosity and σ is the surface tension. The momentum equation in radial direction can be used to conclude this [3, 4]. This is negligible compared to the magnitude of time required for liquid to penetrate the porous medium that is $O(r_o^2\mu/\sigma\sqrt{K})$ with K being the permeability.

Therefore, it is acceptable to ignore the time required for the topology change from sessile droplet to a liquid bridge and define the liquid bridge topology by knowing the volume of the droplet during the contact and the distance between the two surfaces.

III. RESULTS AND DISCUSSIONS

In the first test case a *20 μL* glycerin droplet was deposited on play sand (porosity = *35%*) and a cloth was brought into contact with glycerin. The initial distance was *11 cm.* and the approach speed of the contacting surface was *35 cm/s*. The amount of mass absorbed into the cloth was recorded and compared to the model prediction in Figure 2. The porosity of both surfaces in this case is fairly high and we do not expect much of a spread. That is to say that the amount of spread and footprint of the liquid is a function of the porosity and permeability, the more mass being absorbed into the contacting surface, the less is available to be spread.

A second experiment was conducted by putting a *20 μL* glycerin droplet on kitchen tile with a porosity of *24%*. A wafer of a filtered paper was made in our laboratory with a porosity of *70%* to serve as the secondary surface. Five separate experiments (three repetitions for each experiment) were conducted. The two surfaces were brought into contact

ISBN: 978-988-19253-4-3
ISSN: 2078-0958 (Print); ISSN: 2078-0966 (Online)

after *1, 10, 20, 30,* and *40 minutes,* in which a different amount of glycerin on the surface of the tile was available for transfer into the filter paper wafer. The exerted force was *1 N* for all cases and all experiments started with an initial *2.5 cm* distance between the two surfaces. The amount of transferred glycerin in the secondary surface (wafer) was measured and is compared with the model predictions in Figure 3. These comparisons indicate that the model is fairly accurate in predicting the amount of mass being absorbed into a contacting porous surface.

In another set of validation tests, glass and filter paper were selected as the primary and secondary surfaces, respectively. The two surfaces were brought into contact, and the amount of mass absorbed into the filter paper was measured and compared with the computational model. The initial gap and approach velocity between the two surfaces were similar to the previous test case. These tests were conducted with four different chemicals and the results are depicted in Figure 4. The comparison shows that the model is robust as the physiochemical properties are altered. The presented cases indicate that the model is accurate in predicting the amount of mass that is absorbed when a contact occurs. This is operationally relevant and useful information to assess the amount of threat or contamination.

However, another test case was considered to compare the spread rate in radial direction with absorption or transfer rate into a porous medium. The experimental set-up consists of the same linear stage actuator used for the previous experiments. *200 μL* deionized (DI) water was used as a sessile droplet deposited onto a fused silica optical window, as the impermeable surface, and a porous glass (VykorTM7930) was used as the permeable contacting surface. The physical properties of water are:

$$\mu = 0.001 Pa.s, \rho = 1000 kg/m^3, \sigma = 0.072 N/m.$$

The porous glass has the porosity of *28%* with permeability of 2.08×10^{-19} m^2/s. The surfaces were brought into contact with velocities of *0.5, 1.5, 2.0,* and *2.5 μm/s* and the rate of radius change of the liquid bridge as a function of time was measured. The model input included additional approach velocities of *1.0* and *3.0 μm/s*. In all cases, there is an initial decrease in the radius that is due to the topology transfer from a sessile droplet to a hyperboloid topology.

However, after this initial "*adjustment*" for lower approach velocities, the radius is decreasing in time, meaning that the absorption or capillary transfer is dominating the spread caused by the radial momentum equation. As the approach velocity increases, the momentum equation for the liquid bridge spread in radial direction becomes more dominant, such that the liquid spreads faster than it can be absorbed, causing an increase in the liquid bridge radius. This is important because it provides information regarding the "*extent*" of a contamination in terms of the surface area exposed. The model prediction as compared with experiment is shown in Figure 5.

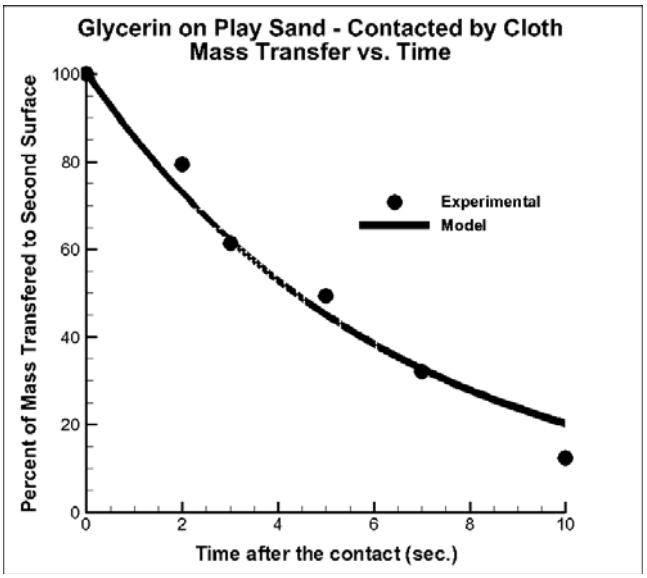

Figure 2: Mass transfer of glycerin initially on sand to cloth by contact as a function of available mass for transfer.

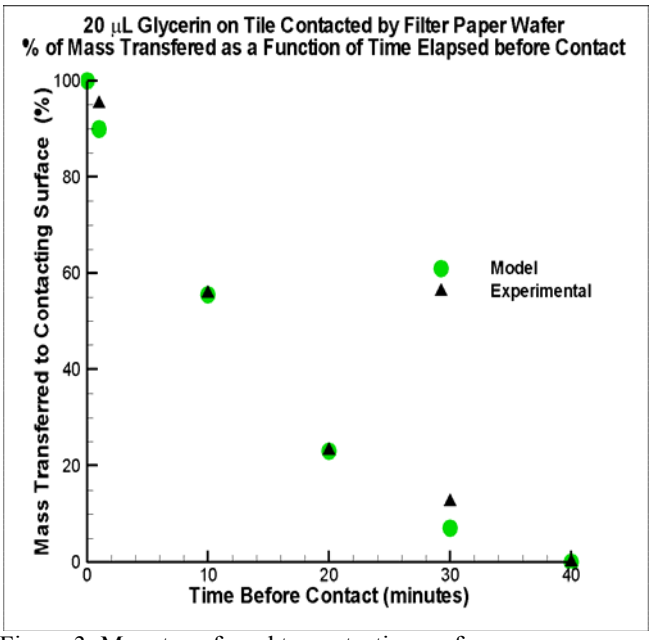

Figure 3: Mass transferred to contacting surface as a function of time elapsed after the contact.

We have presented two cases with chemistry. Model prediction for the degradation of VX on sand due to moisture as compared with experiment is shown in Figure 6. The same scenario is considered as a cloth comes into contact with the primary surface. The contamination of cloth is shown in Figure 7.

ISBN: 978-988-19253-4-3
ISSN: 2078-0958 (Print); ISSN: 2078-0966 (Online)

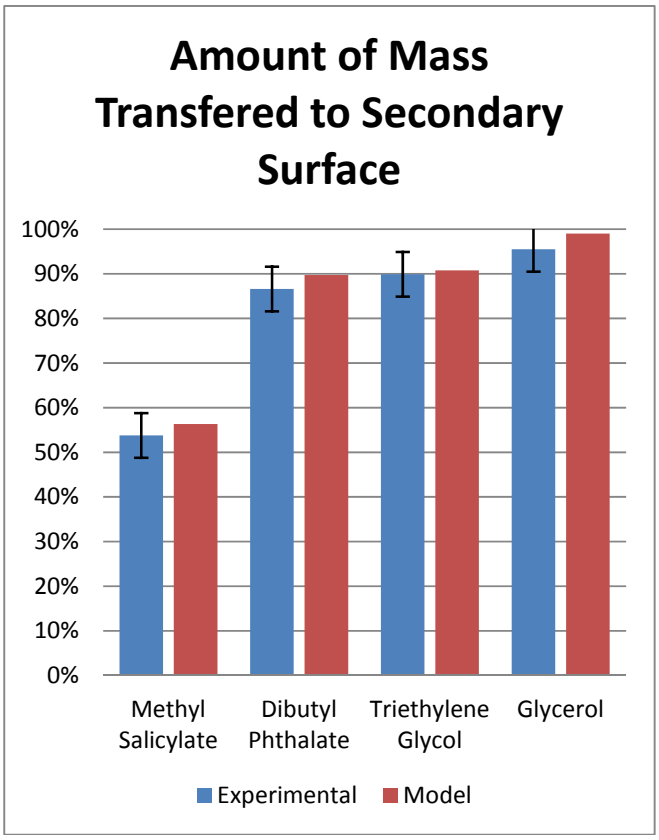

Figure 4: Comparison of model prediction with experimental data for four different chemicals

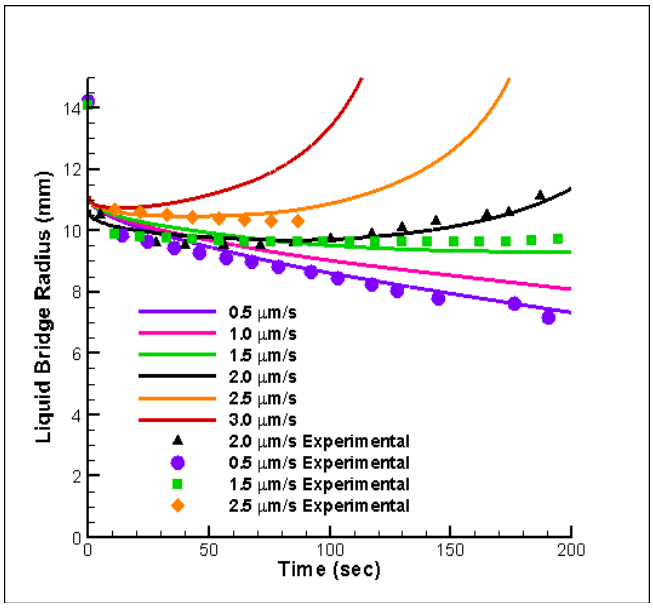

Figure 5: *200 μL* of water on glass contacted by porous glass varied speed of contacting surface.

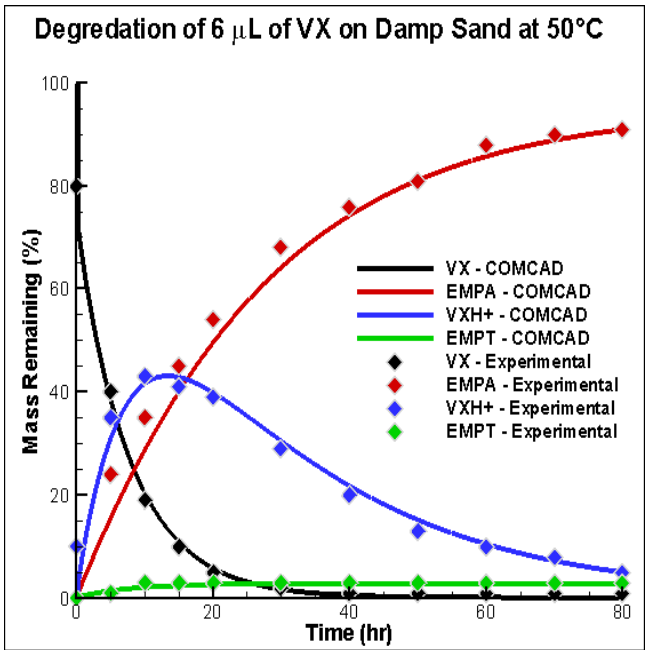

Figure 6: A *6μL* VX droplet undergoes hydrolysis at 50 °C

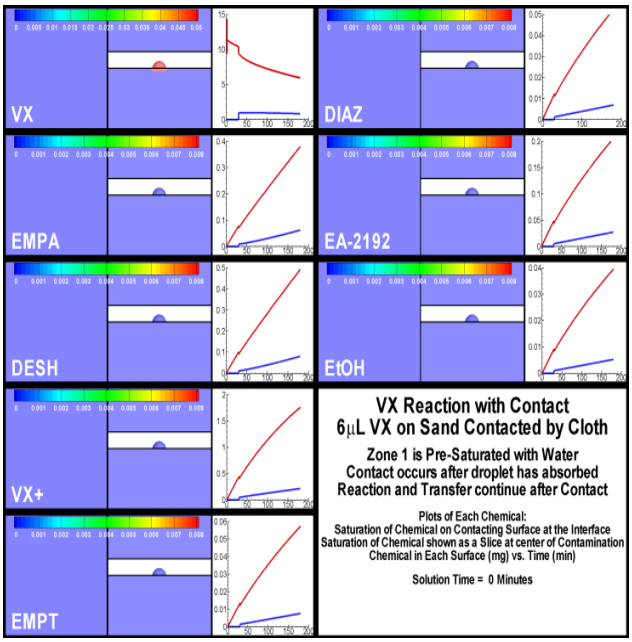

Figure 7: VX on Wet Send and Contact with another Porous Surface

ACKNOWLEDGEMENTS

This research was supported by the Defense Threat Reduction Agency (DTRA) under the contract HDTRA1-10-C-0064. The authors wish to thank the agency for their continued support and vision in the CHEM/BIO Defense area.

ISBN: 978-988-19253-4-3
ISSN: 2078-0958 (Print); ISSN: 2078-0966 (Online)

REFERENCES

[1] Atkinson, T., Navaz, H. K., Zand, A., Jackson, J., Nowakowski, A., "Fate of a Sessile Droplet Absorbed into a Porous Surface Experiencing Chemical Degradation.," *AIChE J*, **60**: 2557–2565, April 2014

[2] Navaz, H.K., Zand, A., Atkinson, T., Gat, A., Nowakowski, A., and S. Paikoff, "Contact Dynamic Modeling of a Liquid Droplet between Two Approaching Porous Materials," *AIChE J.*, **60**: 2346–2353, February 2014

[3] Gat, A., Vahdani, A., Navaz, H., Nowakowski, A., and M. Gharib, "Asymmetric Wicking and Reduced Evaporation Time of Droplets Penetrating a Thin Double-Layered Porous Materials," Applied Physical Letters, **103**, 134104, 2013.

[4] A. Gat, H. K. Navaz, M. Gharib, "Wicking of a Liquid Bridge Connected to a Moving Porous Surface, *Journal of Fluid Mechanics,* 703:315-325., 2012

[5] A. Gat, H. K. Navaz, M. Gharib, "Dynamics of freely moving plates connected by a shallow liquid bridge," *Physics of Fluids,* **23**, 2011

[6] B. Markicevic and H. K. Navaz, "The influence of capillary flow on the fate of evaporating sessile droplet imprint in the porous medium," *Physics of Fluids*, **22**, 1 (2010).

[6] Markicevic, B., and Navaz, H.K., "Primary and secondary droplet spread into porous media," *Transport in Porous Media*, **85**: 953-974, 2010.

[7] B. Markicevic and H. K. Navaz, The influence of capillary flow on the fate of evaporating sessile droplet imprint in the porous medium, *Physics of Fluids*, **22**, Art. No. 122103, (2010).

[8] B. Markicevic, T. G. D'Onofrio and H. K. Navaz, "On Spread Extent of Sessile Droplet into Porous Medium: Numerical Solution and Comparisons with Experiments," *Physics of Fluids*, **22**, Art. No. 012103, 2010.

[9] Markicevic, B. and Navaz, H.K., "Numerical Solution of Wetting Fluid Spread into Porous Media," *International Journal of Numerical Methods for Heat and Fluid Flow*, **19**, 521-534, 2009.

[10] H. K. Navaz, B. Markicevic, A. R. Zand, Y. Sikorski, E. Chan and T. G. D'Onofrio, "Sessile Droplet Spread into Porous Substrates - Determination of Capillary Pressure Using a Continuum Approach," *Journal of Colloid and Interface Science*, **325**, 440-446, 2008.

[11] Navaz, H. K., Chan, E., and Markicevic, B., "Convective Evaporation of Sessile Droplets in a Turbulent Flow – Comparison with Wind Tunnel Data," *International Journal of Thermal Sciences*, **47**, pp. 963-971, 2008.

[12] Navaz, H. K., Markicevic, B., Zand, A., Sikorski, Y., Chan, E., Sanders, M., and D'Onofrio, T., "Sessile Droplet Spread into Porous Substrates – Determination of Capillary Pressure Using a Continuum Approach," *Journal of Colloid and Interface Science,* 325, pp. 440-446, 2008.

[13] Kuo, K. K., (1986), Principles of Combustion, John Wiley and Sons, Chapters 6 and 8.

[14] Vafai, K., Handbook of Porous Media, Marcel Dekker, Inc., Chapter 17, 2000.

[15] Treyball, R. E., Mass-Transfer Operation, McGraw Hill, 1980

ISBN: 978-988-19253-4-3
ISSN: 2078-0958 (Print); ISSN: 2078-0966 (Online)